Electromagnetic Design of a Magnetorheological Damper

Yun-Joo Nam and Myeong-Kwan Park

Journal of Intelligent Material Systems and Structures 2009 20: 181 originally published online 10 June 2008
DOI: 10.1177/1045389X08091117

Electromagnetic Design of a Magnetorheological Damper

YUN-JOO NAM AND MYEONG-KWAN PARK*

Applied Fluid Power Systems Laboratory, Department of Mechanical Engineering
Pusan National University, Busan 609-735, Korea

ABSTRACT: This study presents an electromagnetic design methodology for the magnetorheological (MR) damper. To improve the performance of the MR damper, the magnetic field should be effectively supplied to the MR fluid. Therefore, it is important that the magnetic circuit composed with the MR fluid, the ferromagnetic yoke for forming the magnetic flux path, and the electromagnetic coil are well designed from the electromagnetic viewpoint. For this purpose, two effective approaches are proposed; one is to shorten the magnetic flux path by removing the unnecessary bulk of the yoke in order to improve the static characteristic of the MR damper, and the other is to increase the magnetic reluctance of the magnetic circuit by minimizing the cross-sectional area of the yoke through which the magnetic flux passes in order to improve the dynamic and hysteretic characteristics. After designing and manufacturing two MR dampers, the conventional type and the proposed type, their performances are evaluated and compared through the magnetic field analysis and a series of basic experiments. These results show that the proposed design methodology can be effectively used as a fundamental design material for expanding application fields of the MR damper.

Key Words: magnetorheological fluid, MR damper, electromagnetic design.

INTRODUCTION

A magnetorheological (MR) fluid is a non-colloidal solution composed of ferromagnetic particles with micrometers in diameter dispersed in a nonconductive carrier fluid (Jolly et al., 1999; Phule, 2001). MR fluids have the characteristic that their rheological properties are continuously and reversibly changed within several milliseconds just by applying or removing external magnetic fields. Owing to this feature, MR fluids are increasingly being considered in a large variety of devices, such as shock absorbers (Mikulowski and Holnicki-Szulc, 2003; Norris and Ahmadian, 2003), vibration insulators (Han et al., 2002; Stelzer et al., 2003), brakes or clutches (Carlson et al., 1998; Li and Du, 2003). Compared to conventional actuation methods, devices using the MR fluid can be made simple in construction, high in power, and low in inertia. Especially, the MR fluid actuator can provide more safety in equipment interacted directly with human, due to its inherent stabilizing effect as a passive device. Therefore, the use of the MR fluid actuators is very effective for improving the functions and performances of conventional control systems.

In order to improve the performance of the MR fluid actuator, the magnetic field should be effectively supplied to the MR fluid. While the response time of the MR fluid itself is within several milliseconds, some research has reported that the response time of the MR fluid actuator is relatively slow (An and Kwon, 2003). This is closely related to the electromagnetic properties of the magnetic circuit built in the MR fluid actuator. Especially, the magnetization property of the ferromagnetic yoke in the magnetic circuit leads to the nonlinear input-output relationship of the MR fluid actuator. Therefore, in order to improve the dynamic and hysteretic characteristics of the MR fluid actuator, it is important that the magnetic circuit is well designed from a electromagnetic viewpoint.

Recently, numerous studies on the design of MR dampers have been conducted. In the presence of the magnetic field, MR fluids typically exhibit the similar behavior to a Bingham fluid. It has been reported that the dynamic governing equation of the MR damper derived based on the Bingham plastic model is comparatively practical in real applications. Therefore, the attempts to determine the principal design parameters of the MR damper based on the Bingham plastic model have been made (Bolter and Janocha, 1997; Jolly et al., 1999). However, these studies focused on finding only the mechanical design parameters of the MR damper, and therefore, the electromagnetic properties of the magnetic circuit consisting of the electromagnetic coil, the MR fluid, and the ferromagnetic yoke for

*Author to whom correspondence should be addressed.
E-mail: mkpark1@pusan.ac.kr

1045-389X/09/02 0181–11 $10.00/0 DOI: 10.1177/1045389X08091117

forming the magnetic flux path were not considered adequately in the design phase. In order to overcome this limitation, the magnetic field analysis for the magnetic circuit of the MR damper has been conducted based on the finite element method (FEM) (Gordaninejad et al., 2004; Zhang et al., 2006; Nam and Park, 2007). However, most of the previous studies used the results of the magnetic field analysis to estimate the performance of the MR damper or to verify whether the magnetic saturation occurred or not in the magnetic circuit. In other words, since these results did not analytically provide the design parameters of the magnetic circuit, the approach based on FEM seems not to be a perfect solution for the electromagnetic design of the MR damper. More recently, some attempts to consider the electromagnetic properties of the magnetic circuit in the design of the rotary MR actuator have been made (Takesue et al., 2004; Nam et al., 2007). However, the magnetic circuit of the MR damper has actually many differences from that of the rotary MR actuator in view of the structural configurations and the operating mode of the MR fluid. These differences make it difficult to directly apply the design technique developed for the rotary MR actuator to the MR damper. The research data on the electromagnetic design of the MR damper are currently insufficient and there still remains a wide unexplored domain.

Consequently, the main aim of this study is to propose the electromagnetic design methodology for the MR damper in order to improve its performances. First of all, the principal design parameters are analytically determined considering the electromagnetic properties of the magnetic circuit. Then, through the magnetic field analysis and basic experiments, it is verified that the performance of the MR damper fabricated based on the proposed design methodology is superior to that of the conventional type damper. From these results, it is expected that the proposed design methodology can be effectively used as a fundamental design material for expanding application fields of the MR damper.

MECHANICAL DESIGN OF MR DAMPER

Figure 1 depicts the schematic configuration of the MR damper considered in this work. This MR damper consists of a MR fluid, a casing, a gas accumulator, and a piston head in which the magnetic circuit is installed. The casing is fully filled with the MR fluid and divided into upper and lower chambers by the piston head. When the piston head moves, the MR fluid is moved through the annular gap between the casing and the piston head from one chamber to the other, where the MR fluid is exposed to the applied magnetic field. In order to compensate for changing the fluid volume occupied by the piston rod in the upper chamber,

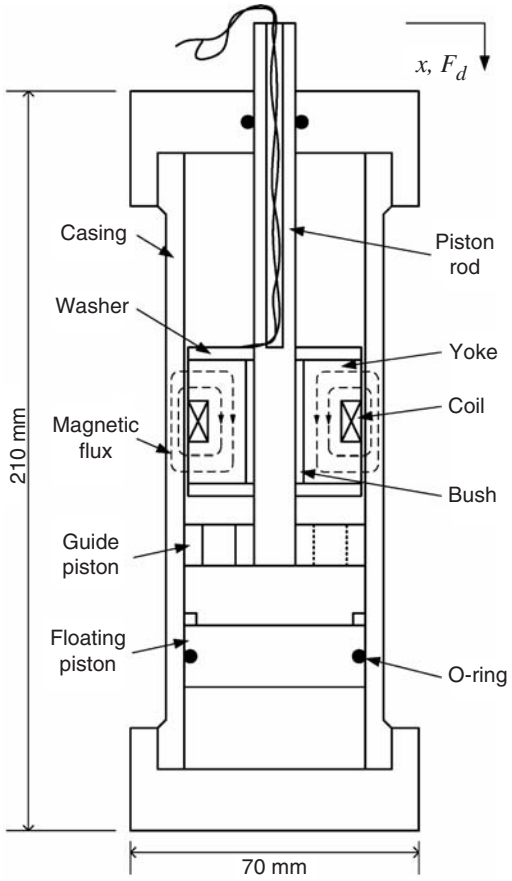

Figure 1. *Schematic configuration of the MR damper.*

the gas accumulator is located in the lower chamber. The magnetic circuit is composed of the MR fluid, the electromagnetic coil, and the ferromagnetic yoke for forming the magnetic flux path. When an external current is supplied to the electromagnetic coil, a magnetomotive force is generated in the magnetic circuit and the corresponding magnetic field is applied to the MR fluid. Then, the dynamic yield stress of the MR fluid is changed depending on the magnetic field intensity, and the resultant damping force is activated in the opposite direction to the motion of the piston head. In the absence of a magnetic field, the damping force occurs only due to the viscosity of the MR fluid itself. However, in the presence of a magnetic field, an additional damping force occurs due to the MR effect of the MR fluid. Therefore, the damping force of the MR damper can be continuously and reversibly controlled by adjusting the coil current.

For the simple but practical design of the MR damper, the following assumptions are introduced: (i) the polar particles are uniformly distributed in the MR fluid without any concentrations, (ii) the flow velocity of the MR fluid is obtained from no slip and linear velocity distribution conditions, (iii) the frictional force is negligible, and (iv) the thermodynamic and inertial effects of the MR fluid can be also disregarded.

Then, the magnetic field-dependent characteristic of the MR fluid can be described using the Bingham plastic model. Although the MR fluid behavior actually exhibits some departures from the Bingham model due to its viscoelastic property, it has been proved by numerous researchers that this simple model is very useful for the design and modeling of MR fluid-based devices (Jolly et al., 1999; Stelzer et al., 2003). Therefore, the constitutive equation for the proposed MR damper can be expressed as (Han et al., 2002; Choi and Wereley, 2003)

$$F_{\mathrm{d}} = F_{\mathrm{MR}} + F_{\eta} + F_{\mathrm{g}} \tag{1}$$

In the above equation, the first term in the right-hand side is the damping force due to the magnetic field-dependent characteristic of the MR fluid (the MR effect):

$$F_{\mathrm{MR}} = (A_{\mathrm{p}} - A_{\mathrm{r}})\frac{2L}{h}\tau_{\mathrm{y}}(H)\,\mathrm{sgn}\,(\dot{x}) \tag{2}$$

where A_{p} is the cross-sectional area of the piston head, A_{r} is the cross-sectional area of the piston rod, L is the total length of the magnetic pole, h is the gap size between the piston head and the casing, H is the magnetic field intensity corresponding to the applied coil current, $\tau_{\mathrm{y}}(H)$ is the dynamic yield stress of the MR fluid corresponding to H, and $\dot{x}$ is the excitation velocity of the piston head. Note that τ_{y} can be obtained from the shear stress–magnetic field intensity curve of the used MR fluid (Lord Corporation, 2003). The second term represents the viscous damping force due to the viscosity of the MR fluid itself:

$$F_{\eta} = \frac{12\eta L_{\mathrm{p}}}{bh^3}(A_{\mathrm{p}} - A_{\mathrm{r}})^2\dot{x} \tag{3}$$

where L_{p} is the total length of the piston head including the magnetic pole L, η is the absolute viscosity of the fluid, and b is the circumference of the piston head. In addition, by assuming that the gas in the accumulator undergoes a polytropic process during operations, the gas spring force F_{g} due to the gas pressure can be given by:

$$F_{\mathrm{g}} = A_{\mathrm{r}}P_{\mathrm{g0}}\left(\frac{V_{\mathrm{g0}}}{V_{\mathrm{g0}} - A_{\mathrm{r}}x}\right)^n \tag{4}$$

where P_{g0} is the initial gas pressure of the accumulator, V_{g0} is the initial volume of the accumulator, x is the displacement of the piston head, and $n \simeq 1.4$ is the polytropic exponent. In the common case, the viscous damping force F_{η} and the gas spring force F_{g} can be considered to be relatively small, compared with the MR effective force F_{MR}. Therefore, the principal design parameters of the MR damper can be effectively determined only by using Equation (2). The maximum magnetic field intensity $H_{\max}$ is constrained by the magnetization property of the MR fluid, and then the maximum yield stress $\tau_{\mathrm{y,max}}$ is determined in the relation of $\tau_{\mathrm{y}}(H_{\max})$. For the convenient fabrication of the MR damper, the gap size h is generally specified in the range of 0.5–2 mm. In addition, the cross-sectional areas A_{p} and A_{r} can be sensibly determined considering the required size and capacity of the MR damper. Then, with the aid of these design parameters, the length of the magnetic pole required for the desired damping force $F_{\mathrm{d,des}}$ can be found by

$$L = \frac{F_{\mathrm{d,des}}h}{2(A_{\mathrm{p}} - A_{\mathrm{r}})\tau_{\mathrm{y,max}}}. \tag{5}$$

ELECTROMAGNETIC DESIGN OF MR DAMPER

In order to improve the performance of the MR damper, the mechanical and electromagnetic designs should be considered simultaneously. In this section, in order to effectively supply the magnetic field to the MR fluid, the electromagnetic design of the magnetic circuit is conducted.

The first target in the design of the magnetic circuit is to increase the magnetic field intensity applied to the MR fluid as much as possible. The increased magnetic field intensity leads to the improvement in the static performance of the MR damper. The relationship between the magnetomotive force generated in the magnetic circuit by applying the coil current and the corresponding magnetic field intensity is given by Ampere's law:

$$NI = \oint_C \mathbf{H}\cdot d\mathbf{l} = H_{\mathrm{f}}l_{\mathrm{f}} + H_{\mathrm{s}}l_{\mathrm{s}} \tag{6}$$

where N is the number of coil turns, I is the coil current, and l is the length of the magnetic flux path. The subscripts f and s represent the physical properties related to the MR fluid and the yoke, respectively. Here, the magnetomotive force NI is constrained by the capacity of the current amplifier available, and the length of the magnetic flux path related to the MR fluid l_{f} is given by $2h$. Moreover, the magnetic field intensity in the yoke H_{s} is upper-bounded by the magnetization property of the used ferromagnetic material. Therefore, in order to increase the magnetic field intensity applied to the MR fluid H_{f}, the length of the magnetic flux path related to the yoke l_{s} should be designed to be minimized.

The second target in the design of the magnetic circuit is to improve its transient response characteristics. As mentioned above, the response of the MR damper is directly influenced by the magnetic response of the

magnetic circuit. The magnetic response characteristic is expressed based on Faraday's law, as:

$$\varepsilon_{\text{inv}} = -\frac{d\phi}{dt} = -L_{\text{s}}\frac{dI_{\text{eddy}}}{dt} = R_{\text{s}}I_{\text{eddy}}$$
$$\Rightarrow I_{\text{eddy}}(t) = I_{\text{eddy},0}\exp\left(\frac{-R_{\text{s}}t}{L_{\text{s}}}\right)$$
$$\Rightarrow \phi(t) = \phi_0\exp\left(\frac{-R_{\text{s}}t}{L_{\text{s}}}\right) \quad (7)$$

where ε_{inv} is the counter electromotive force, ϕ is the magnetic flux passing through the magnetic circuit, and I_{eddy} is the eddy current generated in the magnetic circuit. In addition, L_{s} and R_{s} represent respectively the magnetic inductance and magnetic reluctance of the magnetic circuit, which are dependent on its geometric configuration and the material for the yoke. The subscript 0 represents the initial value of each physical property. When ϕ varies with respect to time, ε_{inv} is generated in the magnetic circuit to prevent the variation of the magnetic flux. Then, I_{eddy} induced on the surface of the magnetic pole by ε_{inv} is converted into Joule heat due to the conductive resistance, and thereafter dissipated with time. This dissipation process is the main cause for the lag of the magnetic response. As can be seen in the above equation, the time constant of the magnetic circuit is $L_{\text{s}}/R_{\text{s}} \propto 1/R_{\text{s}}^2$. Therefore, a practical solution to improve the magnetic response is to increase the magnetic reluctance R_{s} as much as possible. Here, the magnetic reluctance of the magnetic circuit is expressed as:

$$R_{\text{s}} = \frac{l_{\text{s}}}{\mu_{\text{s}}S_{\text{s}}} \quad (8)$$

where μ_{s} is the magnetic permeability of the yoke and S_{s} is the cross-sectional area of the yoke through which the magnetic flux passes. As mentioned above, the length of the magnetic flux path for the yoke l_{s} should be decreased to improve the static performance of the MR damper. Therefore, in order to increase the magnetic reluctance of the magnetic circuit, there is not any alternative except decreasing the cross-sectional area S_{s}. It is notable that decreasing S_{s} also provides an additional effect on decreasing the eddy current itself, due to the increased electric resistance.

In general, the input-output relationship of the MR damper is given by nonlinear and time-varying hysteretic behaviors. The MR fluid exhibits superparamagnetic behavior, in that little or no hysteresis can be observed in its B-H curve (Phule, 2001). On the other hand, the ferromagnetic material for the yoke typically exhibits the nonlinear behavior characterized by magnetic hysteresis loops. In other words, the input-output nonlinearity of the MR damper mainly results from the magnetic hysteresis characteristic of the ferromagnetic material (An and Kwon, 2003). This nonlinearity is undesired because it leads to some distortions in the performances of the MR damper. Therefore, in order to improve the performance of the MR damper as well as to effectively control its damping force, it is necessary that the magnetization properties of the magnetic circuit are considered in the design phase. Actually, due to the open-loop structure of the magnetic circuit, the ferromagnetic material experiences the demagnetization which generates some magnetic field in the direction opposite to that of the magnetization. This demagnetizing field decreases the magnetic field intensity applied to the MR fluid as well as reinforces the magnetic hysteresis of the magnetic circuit. An effective solution to minimize this field is to increase the ratio of the cross-sectional area through which magnetic flux passes to the length of flux path $l_{\text{s}}/S_{\text{s}}$ (Iskander, 1992). Note that this ratio is proportional to the magnetic reluctance of the magnetic circuit. Therefore, it can be concluded that the cross-sectional area should be minimized to improve both the dynamic and the hysteretic characteristics of the magnetic circuit.

On the other hand, the excessive decrease of the cross-sectional area can cause magnetic saturation in the yoke. Therefore, it is necessary to introduce an additional constraint. This constraint is given based on Gauss' law:

$$\phi = \int_S \mathbf{B}\cdot\mathbf{n}dS = B_{\text{f}}S_{\text{f}} = B_{\text{s}}S_{\text{s}} \quad (9)$$

where B_{f} and B_{s} represent the magnetic flux densities of the MR fluid and yoke, respectively. And, S_{f} and S_{s} represent the cross-sectional areas of the MR fluid and yoke, respectively. The maximum magnetic flux density of the MR fluid $B_{\text{f,max}}$ is obtained in accordance with the maximum yield stress $\tau_{\text{y,max}}$, and the saturation magnetic flux density of the yoke $B_{\text{s,sat}}$ is reasonably determined from its magnetization curve. In addition, S_{f} is found by $bL/2$ with the help of Equation (5). Then, in order that the yoke does not experience the magnetic saturation even under the magnetic field corresponding to $B_{\text{f,max}}$, S_{s} should be determined in the following range:

$$S_{\text{s}} \geq S_{\text{s,min}} \equiv \frac{B_{\text{f, max}}S_{\text{f}}}{B_{\text{s, sat}}}. \quad (10)$$

Obviously, some of the previous MR dampers were designed in a similar manner. However, Equation (10) was used to constrain only the cross-sectional area of the magnetic pole being in direct contact with the magnetic fluid, but other geometric parameters of the yoke were determined intuitively at the convenience of manufacturing. Contrarily, in the proposed design methodology, the above condition is used as one constraint for the application of Equations (6)–(8).

Moreover, the selection of the ferromagnetic material for the yoke is very important in the design of the magnetic circuit. This is because the performance of the damper is largely dependent on the magnetization property of the used material, especially the magnetic permeability of the yoke μ_s. However, since further argument is beyond the scope of this work, the material selection problem remains open to future study.

MANUFACTURING OF MR DAMPER

Figure 2 shows the longitudinal cross sections and design parameters of two MR dampers considered in this work: one has the structure similar to a conventional MR damper, and the other is designed based on the proposed design methodology. For convenience, the former is called 'Damper (1)' and the latter is called 'Damper (2)', in this study.

First, the common design parameters of the two MR dampers are determined. The MR fluid used in this work is MRF-132AD composed by Lord Corporation, and the ferromagnetic material for the yoke and the casing is mild steel, SS41. In order to avoid the magnetic saturation in the magnetic materials and to make the input-output relationship of the MR damper as linearly as possible, the values corresponding to about 85% of the actual magnetic saturation are considered for each material. The magnetic properties used in the design of the MR dampers are given in Table 1. Then, with the aid of the minimum cross-sectional area of the yoke $S_{s,\min}$ determined in Equation (10), the outer radius of the casing r_o and the outer radius of the yoke core r_c can be respectively obtained as:

$$r_o = \sqrt{S_{s,\,\min}/\pi + r_i^2} \tag{11}$$

$$r_c = \sqrt{S_{s,\,\min}/\pi + r_b^2} \tag{12}$$

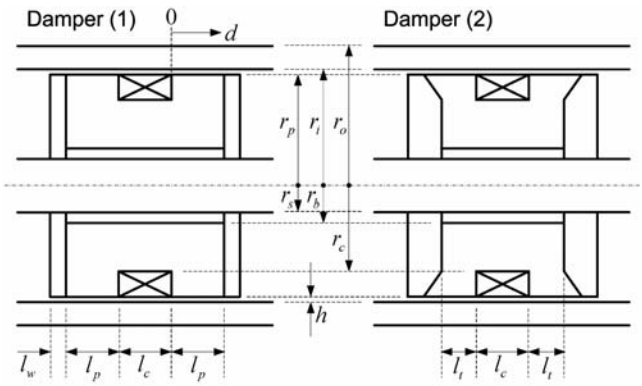

Figure 2. *Design parameters for the MR dampers.*

where r_b is the outer radius of the bush inserted between the piston rod and the position head. Here, the bush is introduced to prevent a direct contact of the yoke with the piston rod and its size is sensibly determined considering the size of the MR damper. In addition, the length of the yoke core l_c can be determined considering the number of coil turns N and the diameter of the used coil d_c. Hereby, all of the design parameters of Damper (1) have been obtained.

As shown in Figure 2, there is one structural difference between the two MR dampers: the yoke flange in the region of $r_c \le r \le r_p$. While the yoke flange of Damper (1) has an identical thickness in the given range, that of Damper (2) is designed by the following design conditions; (i) to minimize the cross-sectional area of the yoke through which the magnetic flux passes while the magnetic saturation does not occur and (ii) to remove the unnecessary bulk of the yoke in order to shorten the magnetic flux path. According to these conditions, the desired thickness of the yoke flange can be given by

$$l = \frac{S_{s,\,\min}}{(2\pi r)} \quad \text{for} \quad r_c \le r \le r_p. \tag{13}$$

From the above equation, the thickness of the flange at $r = r_c$ can be obtained as $l_t = S_{s,\,\min}/(2\pi r_c)$. On the other hand, in order to obtain the desired damping force of the MR damper, the length of the magnetic pole $l_p = L/2$ should be determined by Equation (5). This may not be consistent with the thickness of the flange at $r = r_p$ obtained from the above equation, $l_p = S_{s,\,\min}/(2\pi r_p)$. In other words, for the desired capacity (2000 N) of the MR damper considered in this work, the surface area of the magnetic pole is unavoidably designed to be wider than $S_{s,\min}$. If the desired damping force is set to be relatively small, its opposite can be true. This disagreement is because of the difference in the magnetic permeability between the MR fluid and the yoke. Nevertheless, in order to make the cross-sectional area as small as possible, the geometric configuration of the magnetic circuit in Damper (2) is proposed as shown in Figure 2. This structure seems to be effective to increase the magnetic field intensity applied to the MR fluid by shortening the flux path as well as to lead to the smooth

Table 1. Properties of the magnetic materials used for the MR dampers.

Property	Value	Material
$\tau_{y,max}$	38.28 kPa	MRF-132AD for MR fluid (Lord Corporation, 2003)
$B_{f,max}$	0.676 T	
η_f	150 A/mm	
$B_{s,sat}$	1.326 T	SS41 steel for yoke (An and Kwon, 2003)
$H_{s,sat}$	1.989 A/mm	

variation of the magnetic flux density. This is particularly helpful in reducing the weight of the MR damper itself. The design specifications of the two MR dampers are given in Table 2. The external appearances of the manufactured dampers are shown in Figure 3. Here, the bush and the washer employed for preventing leakage of magnetic field as well as the guide piston with the porous structure are made of MC nylon which is a kind of nonconductive and nonmagnetic materials. The full stroke of the MR dampers is 80 mm.

MAGNETIC FIELD ANALYSIS FOR MR DAMPER

In order to examine the effectiveness of the proposed design methodology, the magnetic field analysis is conducted. Figure 4 shows the magnetic flux density distributions of the two dampers at the coil current of 5 A which is the maximum value available. As expected above, the magnetic flux densities of the two dampers are somewhat diluted between the magnetic pole and the MR fluid, due to the difference of the magnetic permeability. Nevertheless, it can be clearly seen that the magnetic flux density in Damper (2) is more uniformly distributed than that in Damper (1). This results from the minimization of the cross-sectional area through which the magnetic flux passes. Therefore, it is expected that the performances of Damper (2) are superior to that of Damper (1), in perspective of the dynamic and hysteretic characteristics.

Moreover, Figure 5 shows the magnetic field intensities with respect to the location d (this variable is depicted in Figure 2) on the magnetic pole. The magnetic field intensities monotonously decrease with the increase of the location. This is because the magnetic flux path is shorter as it is closer to the electromagnetic coil. Note that the values corresponding to 85% of the actual maximum magnetic saturation were used in the design phase. Otherwise, this variation of the magnetic filed intensity might cause the magnetic saturation near the electromagnetic coil. Obviously, it is verified from Figure 4 that the magnetic flux densities of both dampers do not exceed the actual saturation value of the yoke, 1.56 T. In addition, it can be seen from Figure 5 that the magnetic field intensity of

Table 2. Design parameters of the MR dampers.

Parameters	Symbol	Value
Desired damping force	F_{des}	2000 N
Available maximum current	I_{max}	5.0 A
Coil turn number	N	80
Gap size	h	1.0 mm
Inner radius of the casing	r_i	22.0 mm
Outer radius of the casing	r_o	26.4 mm
Outer radius of the piston	r_p	21.0 mm
Radius of the piston rod	r_s	5.0 mm
Outer radius of the bush	r_b	7.0 mm
Radius of the yoke core	r_c	16.2 mm
Length of the magnetic pole	l_p	10.0 mm
Length of the yoke flange	l_t	6.6 mm
Length of the yoke core	l_c	10.0 mm
Coil diameter	–	0.5 mm
Electric resistance of the coil	–	1.24 Ω
Initial gas pressure	P_{g0}	10 bar
Initial gas volume	V_{g0}	11634 mm^3

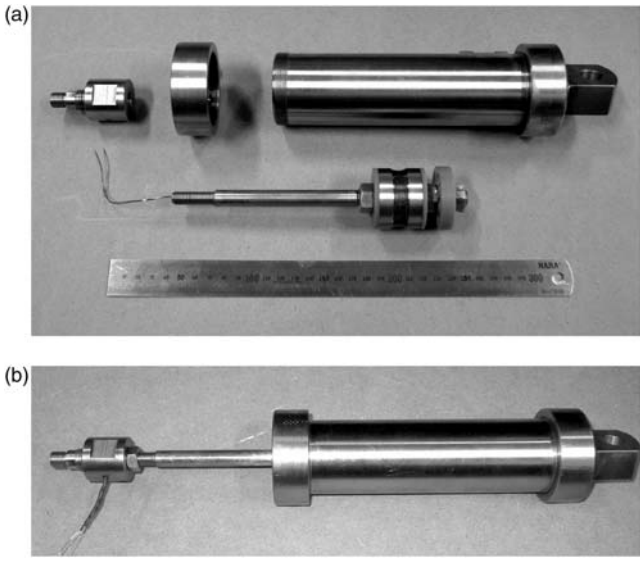

Figure 3. *Appearances of the MR damper. (a) Parts, (b) Assembly.*

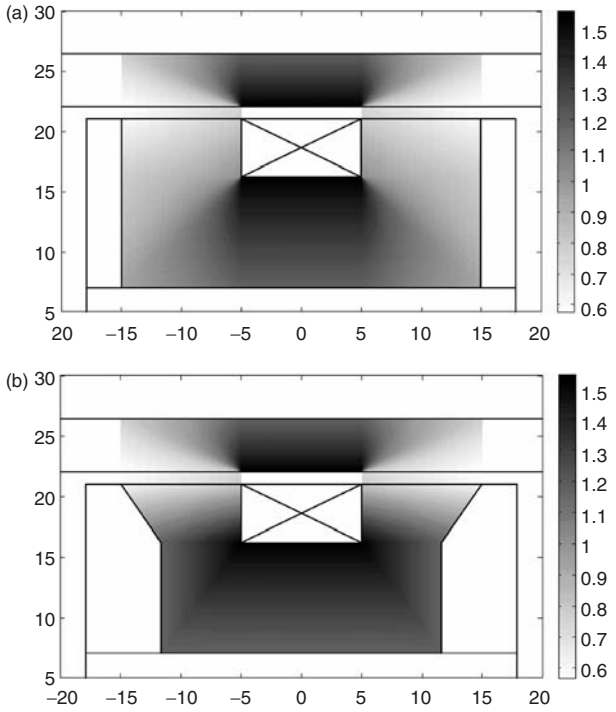

Figure 4. *Magnetic flux density distributions (unit in the scale bar: tesla) (a) Damper (1), (b) Damper (2).*

Damper (2) is slightly larger than that of Damper (1). This implies that the proposed design methodology can be effective for improving the static characteristic of the MR damper. Nevertheless, there is no remarkable difference in the average magnetic field intensity between the two dampers. This is because the length of the magnetic pole determined by Equation (5) is inevitably larger than that required in Equation (11). In other words, the capacity and size of the MR damper considered in this work limit to exactly apply the proposed design methodology. When the diameter of the piston head is increased so that the length of the magnetic pole required for the desired damping force is decreased, this limitation can be solved effectively, leading to the further improved static performance of the damper. The further argument on the optimization of the design parameter for the MR damper is beyond the scope of this work. Therefore, this problem remains open to future study.

PERFORMANCE EVALUATION OF MR DAMPER

Figure 6 shows the experimental apparatus constructed to evaluate the performances of the fabricated MR dampers. The MR damper is excited at a certain velocity by a hydraulic cylinder. Here, a proportional hydraulic valve is employed to keep the excitation velocity of the hydraulic cylinder constant even in the presence of the damping force of the MR damper. The coil current input to the MR damper can be adjusted by the current amplifier which can be controlled by the personal computer with the DC converter. During operations, the damping force and displacement of the MR damper are measured by a loadcell mounted on the base frame and a linear potentiometer connected with the hydraulic cylinder, respectively. The sensor signals are transmitted to the personal computer via the AD converter with its sampling frequency of 1000 Hz.

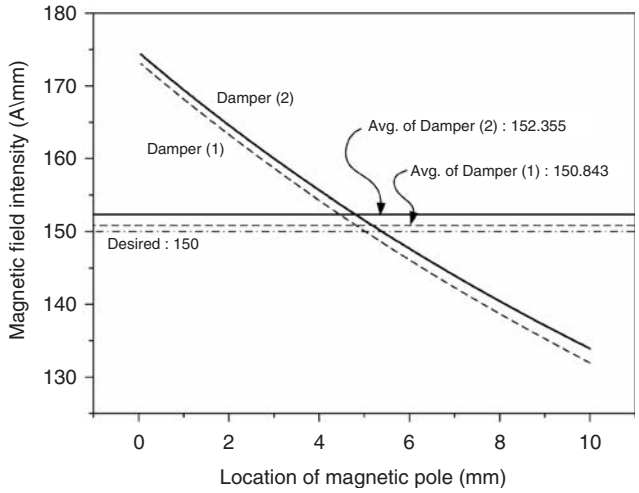

Figure 5. *Magnetic field intensities on the magnetic pole.*

Static Characteristics

For the evaluation of the static characteristics, the MR damper is initially positioned at its displacement of 20 mm. After the coil current is applied at a specified level, the MR damper is oscillated in a triangular waveform with various excitation frequencies at a constant excitation amplitude of 20 mm.

Figure 7 shows time histories of the damping forces under various coil currents at the excitation velocity of 0.262 m/s, which is an example of the experimental results. Figure 8 shows the damping force–excitation velocity curves of the two dampers, which are obtained from the maximum damping forces measured at different velocities. It can be seen from this figure that the damping forces of the presented MR dampers can be effectively controlled with the coil current. The damping force is somewhat increased with the increase of the excitation velocity at a specified current, which is due to the viscosity of the MR fluid itself. Its increasing rate is relatively small and nearly independent of the applied coil currents, as expected in the mechanical design phase. These damping characteristics result from the Bingham behavior of the MR fluid in the presence of magnetic fields.

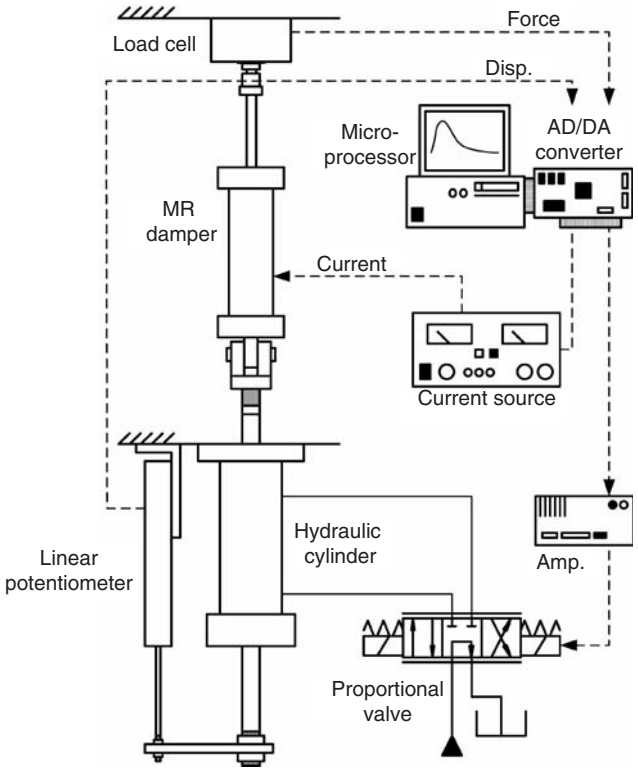

Figure 6. *Experimental apparatus.*

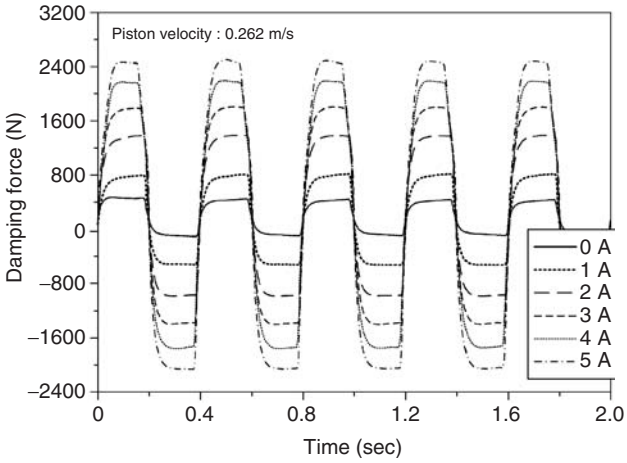

Figure 7. *Damping force histories with respect to the coil currents.*

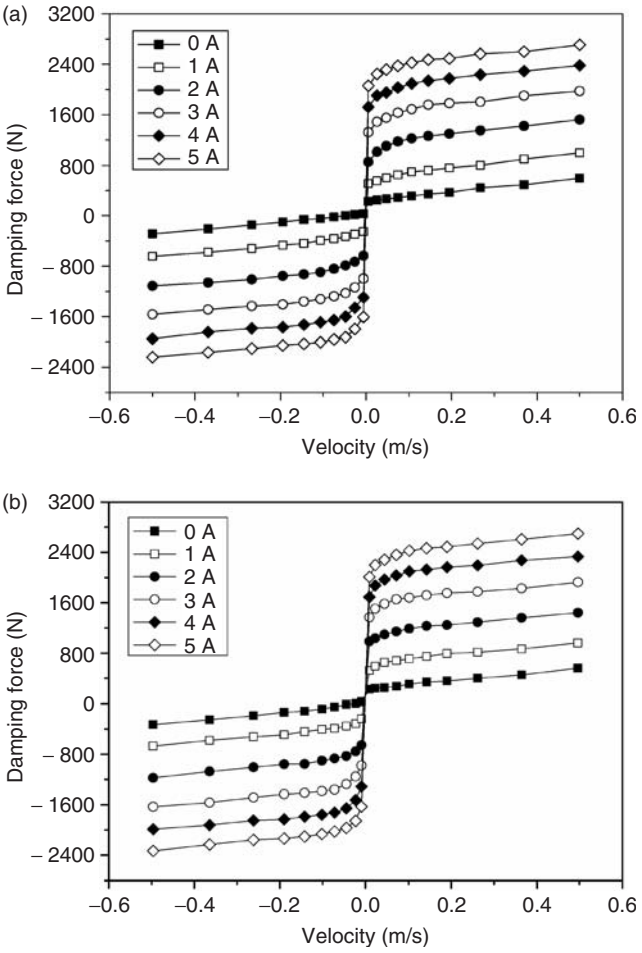

Figure 8. *Static characteristics (a) Damper (1), (b) Damper (2).*

For further discussion, Figure 9 shows the comparison result between the analytical and predicted models for the damping force. Here, the analytical model is obtained by curve-fitting the measured results with the Bingham model and the predicted model is calculated by using Equation (1). The analytical

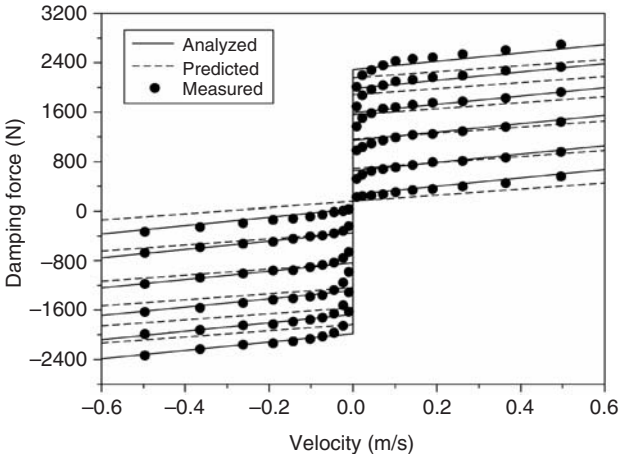

Figure 9. *Comparison between the analytical and predicted damping force models.*

model has slightly larger viscous damping force than the predicted one; $F_\eta = 702.18\dot{x}[N]$ for the analytical model and $F_\eta = 582.02\dot{x}[N]$ for the predicted one. This difference is considered to result from the viscous frictional force due to the oil seals and the guide piston. Also, the static frictional force is found to be $\approx$63 N, which is in order of a negligible level. Despite some departures, the predicted model is in good agreement with the analytical (or measured) one. Therefore, it can be concluded that Equation (1) derived based on the Bingham model is very useful for the design and modeling of the MR dampers.

In order to effectively compare the magnetic field-dependent characteristics of the two dampers, the MR effective damping forces with respect to the coil currents are depicted in Figure 10. As expected in the magnetic field analysis, it is verified that the static damping characteristics of the two dampers are nearly identical to each other. If the yoke is designed to have the multi-magnetic poles so that the mechanical and electromagnetic design conditions are simultaneously satisfied, the significant improvement in the static characteristics is expected. Future studies will be focused on this achievement. On the other hand, it is remarkable that the presented dampers exhibit good linearity between the MR effective damping force (output) and the coil current (input); $F_{\mathrm{MR}} = 426.8I - 3.83[N]$. This is because the values corresponding to about 85% of the actual maximum magnetic saturation were used in the design of the MR dampers. Therefore, it is expected that the MR dampers presented in this work can be used in a variety of the practical force control applications.

Dynamic Characteristics

Figure 11 shows the step responses of the damping force to step input currents, from which the dynamic characteristics of the presented MR dampers

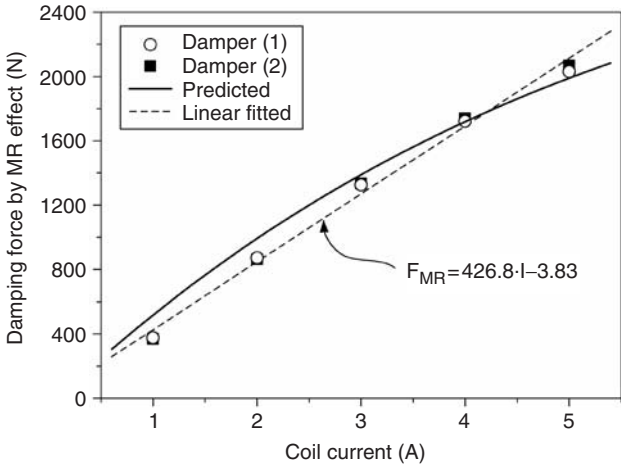

Figure 10. *Comparison of the MR effects: damping force vs. coil current.*

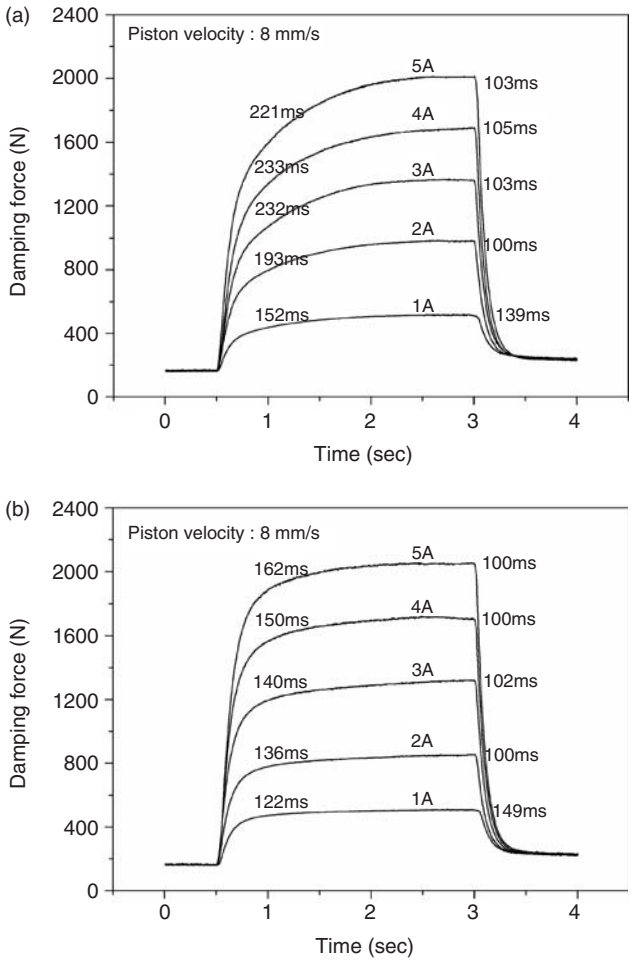

Figure 11. *Step response characteristics. (a) Damper (1), (b) Damper (2).*

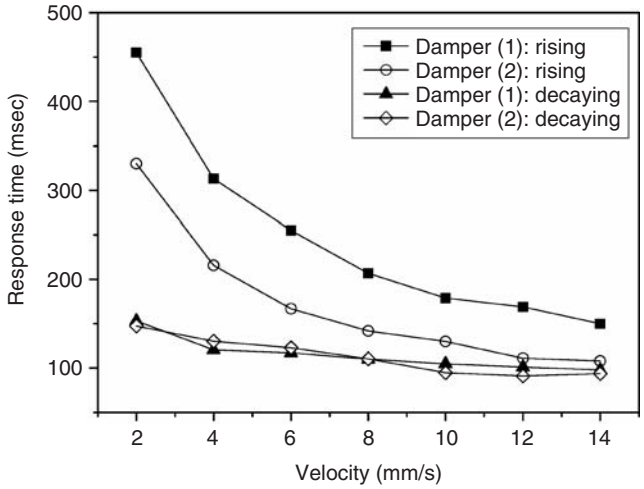

Figure 12. *Response times with respect to the piston velocities.*

can be examined. The displacement of the dampers is initially set to 20 mm. As the damper is compressed at the excitation velocity of 8 mm/s, the current is input at the instance of 0.5 s, and then removed at the instance of 3.0 s. In general, the damping force of the MR damper under the step input current exhibits the dynamic behavior similar to the first-order linear system. In other words, the rising response time is defined as the time required for the damping force to reach 63.2% of its saturated value after the current has been switched on. Similarly, the decaying response time can be defined as the time required for the saturated damping force to decline to 36.8% after the current has been switched off. Through the comparison study between the simulation analysis and the experimental result, the average time constants of rising responses for Dampers (1) and (2) are found to be ≈206.2 and 142.0 ms, respectively. In addition, the measured decaying times are found to be ≈110 ms, nearly irrespectively of the applied currents.

On the other hand, Figure 12 shows the effect of the piston velocity on the response times. Some of the previous scientific researches has verified that (i) at the same fluid flow condition, the rising time of the MR fluid is larger than the decaying time (Yoshida et al., 2002), and (ii) the rising and decaying times tend to be exponentially decreased with the increase of the flow rate or shear rate (Koo et al., 2006). In other words, the decaying responses of the MR damper are determined only by the hydrodynamic force acting on the MR fluid, while the rising responses are determined in the interaction between the field-induced particle attractive force and the hydrodynamic force. Obviously, the experimental results obtained in this study well agree with the above statements. Especially, it can be seen that the rising response times of Damper (2) are significantly smaller than those of Damper (1). The improvement in the dynamic characteristic is considered to be obtained by minimizing the cross-sectional area through which the magnetic flux passes. Therefore, it is proved that the proposed electromagnetic design methodology is effective for improving the dynamic response characteristic of the MR damper.

Hysteretic Characteristics

Figure 13 shows the experimental results conducted to examine the hysteretic characteristics of the MR dampers, where the measured damping forces are normalized with the minimum and maximum values for the effective comparison between the two dampers. The initial displacement of the MR damper is set to 20 mm. When compressing the MR damper at the excitation velocity of 8.0 mm/s, the current is varied from 0 through 5 to 0 A, in a triangular waveform with its period of 4 s. The nonlinearities of Dampers (1) and (2) are about 15.7 and 14.1%, respectively. In this study, the nonlinearity is simply defined as a measure of the maximum deviation of the calibration curve from a straight line drawn between no-force and full-scaled force outputs, expressed as a percentage of the full-scale output. In addition, it is verified through additional experiments (Figure 14) that the hysteretic characteristics of the presented MR dampers are nearly independent of the excitation velocities.

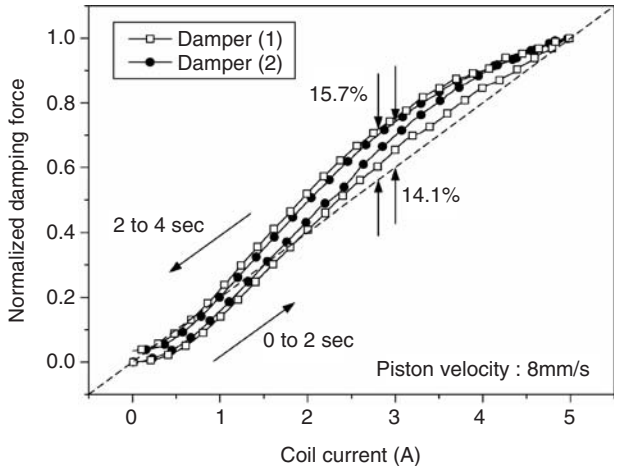

Figure 13. *Hysteretic characteristics.*

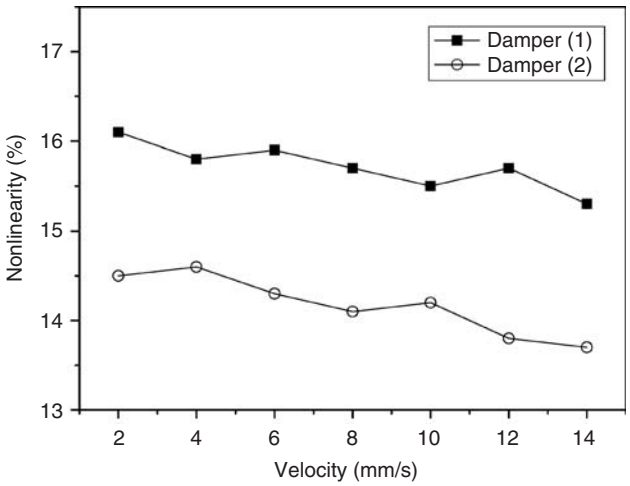

Figure 14. *Nonlinearities with respect to the piston velocities.*

From the results, it can be seen that Damper (2) exhibits better hysteresis characteristics than Damper (1), which result from minimizing the cross-sectional area of the yoke in order to reduce the demagnetizing fields. Therefore, it is proved that the proposed electromagnetic design methodology is effective for improving the hysteretic characteristic of the MR damper.

CONCLUSIONS

In this study, an electromagnetic design methodology for the magnetic circuit of the MR damper is proposed to improve the performances of the damper. Through the magnetic field analysis and basic experiments, its effectiveness is verified. The results obtained in this work can be summarized as:

1. The static characteristic of the MR damper can be slightly improved by removing the unnecessary bulk of the yoke in the magnetic circuit in order to shorten the magnetic flux path.
2. The dynamic and hysteretic characteristics of the MR damper can be significantly improved by reducing the cross-sectional area of the yoke through which the magnetic flux passes in order to increase the magnetic reluctance of the magnetic circuit.
3. It was verified that the performances of the electromagnetically designed MR damper is superior to those of the conventional type MR damper. Therefore, the proposed design methodology is effective for the design of the MR damper.
4. It is expected that the proposed electromagnetic design methodology can be used as a fundamental material for expanding application fields of the MR damper.

REFERENCES

An, J. and Kwon, D.S. 2003. "Modeling of a Magnetorheological Actuator Including Magnetic Hysteresis," *Journal of Intelligent Material Systems and Structures*, 14(9):541–550.

Bolter, R. and Janocha, H. 1997. "Design Rules for MR fluid Actuators in Different Working Modes," *Proceedings in SPIE Symposium on Smart Structures and Materials*, pp. 148–159.

Carlson, J.D., Leroy, D.F. and Marjoram, R.H. 1998. "Controllable Brake," US Patent 5842547.

Choi, Y.T. and Wereley, N.M. 2003. "Vibration Control of a Landing Gear System Featuring Electrorheological/Magnetorheological Fluids," *Journal of Aircraft*, 40(3):432–439.

Gordaninejad, F., Wang, X., Hitchcock, G., Bangrakulur, K., Fuchs, A., Elkins, J., Evrensel, C., Ruan, S., Siino, M. and Kerns, M. 2004. "A New Modular Magneto-Rheological Fluid Valve For Large-Scale Seismic Applications," *Proceedings in the Fourth International Workshop on Structural Control*, pp. 140–145.

Han, Y.M., Nam, M.H., Han, S.S., Lee, H.G. and Choi, S.B. 2002. "Vibration Control Evaluation of a Commercial Vehicle Featuring MR Seat Damper," *Journal of Intelligent Material Systems and Structures*, 13(9):575–579.

Iskander, M.F. 1992. *Electromagnetic Fields and Waves*, Englewood Cliffs NJ, Prentice Hall.

Jolly, M.R., Bender, J.W. and Carlson, J.D. 1999. "Properties and Applications of Commercial Magnetorheological Fluids," *Journal of Intelligent Material Systems and Structures*, 10(1):5–13.

Koo, J.H., Goncalves, F.D. and Ahmadian, M. 2006. "A Comprehensive Analysis of the Response Time of MR Dampers," *Smart Materials and Structures*, 15:351–358.

Li, W.H. and Du, H. 2003. "Design and Experimental Evaluation of a Magnetorheological Brake," *International Journal of Advanced Manufacturing Technology*, 21(7):508–515.

Lord Corporation. 2003. "MagnetoRheological Fluid MRF-132AD," Product Bulletin.

Mikulowski, G. and Holnicki-Szulc, J. 2003. "Adaptive Aircraft Shock Absorbers," *AMAS Workshop on Smart Materials and Structures*, SMART'03, pp. 71–80.

Nam, Y.J. and Park, M.K. 2007. "Performance Evaluation of Two Different Bypass-Type MR Shock Dampers," *Journal of Intelligent Material Systems and Structures*, 18(7):707–717.

Nam, Y.J. Moon, Y.J. and Park, M.K. 2007. "Performance Improvement of a Rotary MR Fluid Actuator Based on Electromagnetic Design," *Journal of Intelligent Material Systems and Structures* 2008 19:695–705.

Norris, J.A. and Ahmadian, M. 2003. "Behavior of Magneto-Rheological Fluids Subject to Impact and Shock Loading," *ASME International Mechanical Engineering Congress and Exposition*, IMECE'03, pp. 1–6.

Phule, P. 2001. "Magnetorheological (MR) Fluid: Principles and Applications," *Smart Materials Bulletin*, 2001(2):7–10.

Stelzer, G.J., Schulz, M.J., Kim, J. and Allemagn, J. 2003. "A Magnetorheological Semi-Active Isolator to Reduce Noise and Vibration Transmissibility in Automobiles," *Journal of Intelligent Material Systems and Structures*, 14(2):743–765.

Takesue, N., Furusho, J. and Kiyota, Y. 2004. "Fast Response MR-Fluid Actuator," *JSME International*, Part C, 47(3):783–791.

Yoshida, K., Takahashi, H., Yokota, S., Kawachi, M. and Edamura, K. 2002. "A Bellows-Driven Motion Control System Using A Magneto-Rheological Fluid," *Proceedings in the Fifth JFPS International Symposium on Fluid Power*, pp. 403–408.

Zhang, H.H., Liao, C.R., Chen, W.M. and Huang, S.L. 2006. "A Magnetic Design Method of MR Fluid Dampers and FEM Analysis on Magnetic Saturation," *Journal of Intelligent Material Systems and Structures*, 17(8–9):813–818.